



Near-Infrared Fluorescence Imaging and Photodynamic Therapy for Liver Tumors

Masaki Kaibori*, Hisashi Kosaka, Kosuke Matsui, Morihiko Ishizaki, Hideyuki Matsushima, Takumi Tsuda, Hidehiko Hishikawa, Tadayoshi Okumura and Mitsugu Sekimoto

Department of Surgery, Kansai Medical University, Osaka, Japan

OPEN ACCESS

Edited by:

John Russell Benson,
Cambridge University Hospitals NHS
Foundation Trust, United Kingdom

Reviewed by:

Jai Young Cho,
Seoul National University Bundang
Hospital, South Korea
Takeshi Aoki,
Showa University Hospital, Japan

*Correspondence:

Masaki Kaibori
kaibori@hirakata.kmu.ac.jp

Specialty section:

This article was submitted to
Surgical Oncology,
a section of the journal
Frontiers in Oncology

Received: 06 December 2020

Accepted: 05 February 2021

Published: 25 February 2021

Citation:

Kaibori M, Kosaka H, Matsui K,
Ishizaki M, Matsushima H, Tsuda T,
Hishikawa H, Okumura T and
Sekimoto M (2021) Near-Infrared
Fluorescence Imaging and
Photodynamic Therapy for Liver
Tumors. *Front. Oncol.* 11:638327.
doi: 10.3389/fonc.2021.638327

Surgery with fluorescence equipment has improved to treat the malignant viscera, including hepatobiliary and pancreatic neoplasms. In both open and minimally invasive surgeries, optical imaging using near-infrared (NIR) fluorescence is used to assess anatomy and function in real time. Here, we review a variety of publications related to clinical applications of NIR fluorescence imaging in liver surgery. We have developed a novel nanoparticle (indocyanine green lactosome) that is biocompatible and can be used for imaging cancer tissues and also as a drug delivery system. To date, stable particles are formed in blood and have an ~10–20 h half-life. Particles labeled with a NIR fluorescent agent have been applied to cancer tissues by the enhanced permeability and retention effect in animals. Furthermore, this article reviews recent developments in photodynamic therapy with NIR fluorescence imaging, which may contribute and accelerate the innovative treatments for liver tumors.

Keywords: near-infrared fluorescence imaging, liver surgery navigation, photodynamic therapy, liver tumors, indocyanine green lactosome

INTRODUCTION

Many imaging tools, including ultrasonography (US), positron emission tomography (CT), and magnetic resonance imaging (MRI), are used and necessary for recent hepatic surgery. However, these imaging treatments can be insufficient for detecting smaller tumors, which require more high spatial resolution than these methods have. For clinical use, real-time cancer detection with fluorescence probes, such as indocyanine green (ICG) and the porphyrin precursor, 5-aminolevulinic acid (5-ALA), is an important topic. ICG and 5-ALA are appropriated as fluorescence imaging (FI) agents, but their application is inadequate for certain diseases. After ICG injection, intraoperative fluorescent angiography has been performed to evaluate the patency of coronary artery bypass grafts (1–4). The use of intraoperative FI can reportedly allow better visualization during hepatobiliary surgery (5). ICG can bind to plasma proteins and affect its fluorescence, emitting near-infrared (NIR) light (6, 7). Proteins in human bile also bind to ICG (8). Prior to hepatic surgery, ICG is administered to measure the ICG retention time (ICGR15; at 15 min), estimating the maximum hepatic volume that can be safely resected (9, 10). Many high-volume hepatectomy centers in Japan are beginning to use ICG FI for intraoperative navigation, such as visualizing small liver tumors, cholangiography, and imaging hepatic segments.

Remarkable advances in photodynamic therapy (PDT) for liver tumors have also been reported. Development of molecular probes based on nanoparticles, polymer micelles that use the characteristics of neovascularization, is currently underway. By including various signaling agents (e.g., radioisotopes, fluorescent agents, magnetic substances) in the nanoparticles, diagnosis can be made by molecular imaging of new vascular tissue. If a therapeutic agent is included, this method may also provide a drug delivery system. Theranostics (a fusion of “diagnostics” and “therapy”) can be realized (11) and may lead to ultra-early cancer diagnosis and treatment.

We used the enhanced permeability and retention characteristics of neovascularization (12), which are prominent in inflammatory diseases such as rheumatoid arthritis, ischemic diseases such as arteriosclerosis, and initial cancer growth. Here, we review features of NIF FI and photodynamic therapy for liver tumors.

NEAR-INFRARED FLUORESCENCE IMAGING DURING LIVER SURGERY NAVIGATION

Tumor Visualization

Gotoh et al. (13) and Ishizawa et al. (14) reported the novel technics for liver cancers with ICG fluorescence image (FI) navigation, which is based on the capacity of hepatocellular carcinoma (HCC) to accumulate ICG. ICG was injected several days before surgery. ICG FI found the HCC tumors that were completely removed, with negative margins, using the FI as a guide. It is essential to detect small HCCs for curative resection and improvement of patient outcomes. Further strong definition between tumor and non-tumor cells is essential for obtaining safe surgical margins. The authors showed that FI following pre-operative intravenous injection of ICG confirmed HCCs and colorectal liver metastases (CRLM) on cut surfaces of resected specimens in 37 patients with HCC and 12 with CRLM (14). There were three types of fluorescence patterns in tumors: (i) total, all tumor tissue showed uniform fluorescence; (ii) partial, some showed fluorescence; and (iii) rim, the surrounding liver parenchyma except cancer tissues showed fluorescence. Total-type tumors contained all well-differentiated HCCs, while rim-type tumors contained poorly differentiated HCCs and CRLM. In addition to detecting the small HCCs, ICG-FI was reportedly useful for the detection of CRLM (15, 16), peritoneal dissemination (17, 18), and lymph node metastasis from HCC (19).

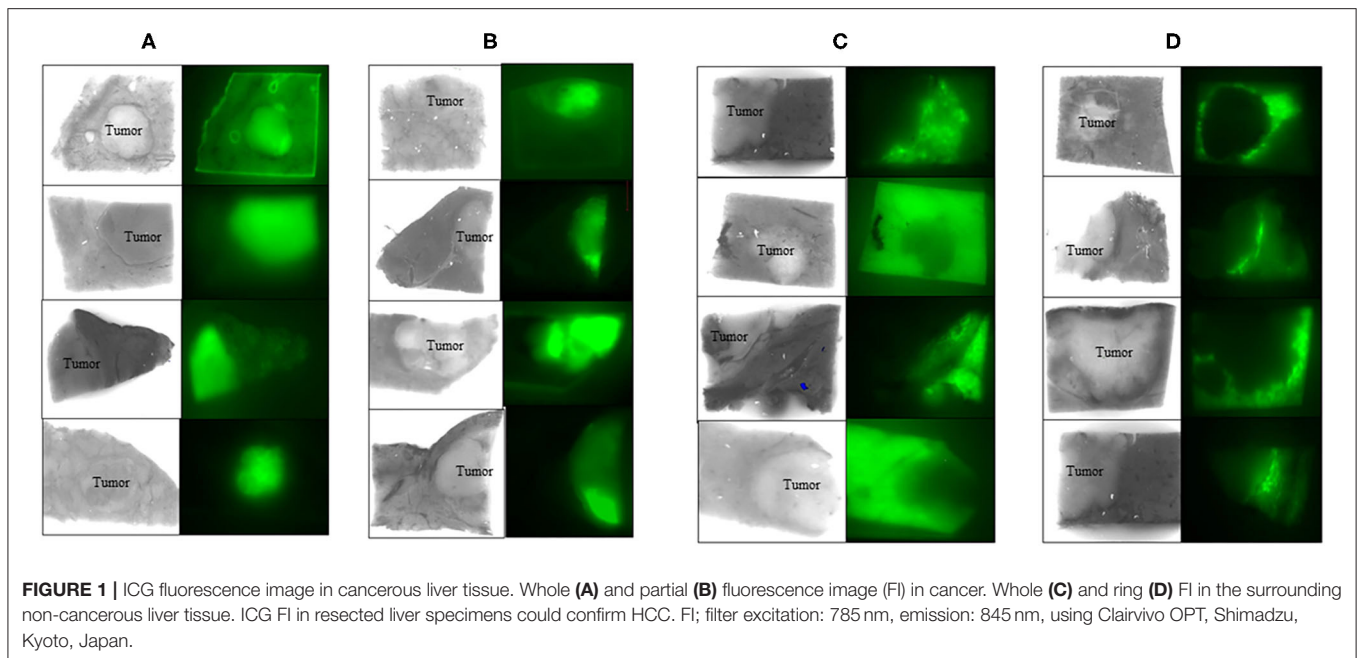
The mechanism of ICG-FI for HCC has been revealed by gene expression and histochemical staining analyses (20). The expression of portal uptake transporters of ICG, which are organic anion-transporting polypeptide-8 and Na⁺/taurocholate

cotransporting polypeptide (21), were well-maintained in differentiated HCC tissues. However, functional biliary excretion was disordered, which was followed by ICG retention in cancerous tissues at the time of surgery. In contrast, portal uptake transporters were downregulated in poorly differentiated HCCs and biliary excretion of ICG by surrounding non-cancerous hepatic parenchyma was disordered, resulting in rim-type fluorescence. In CRLM, the rim-type fluorescence signal is reportedly found by immature hepatocytes with reduced bile excretion (22).

We reported that ICG FI for HCC is effective for both assessing tumor differentiation and detecting fibrosis in non-cancerous liver parenchyma (23). We evaluated ICG FI of resected specimens from 190 HCC patients. This system (fluorescence image; using Clairvivo OPT, Shimadzu, Kyoto, Japan) consisted of a horizontal sample table, excitation light sources, charge-coupled device camera, camera lens, optical filter, and white laser-emitting diode light sources that illuminated the sample from four angles. They were classified into two groups: high cancerous [HC] and high surrounding [HS] groups, according to FI (Figure 1). These groups were further sub-classified into whole and partial types (Figures 1A,B), and whole and ring types (Figures 1C,D), respectively. The patients in the HC group had a higher prevalence of esophageal or gastric varices, and worse liver function than those in the HS group. The HC group also had a higher percentage of limited resection cases as compared with the HS group. Cirrhotic liver histology was more common in the HC group than in the HS group. In multivariate analysis, HC status was a predictive factor for cirrhosis in HCC patients. In the HC group, a higher number of well-differentiated HCC cases was seen in the partial-type subgroup [23/48 (48%), Figure 1A] than in the whole-type subgroup [7/68 (10%), Figure 1B]. In the HS group, a higher number of poorly differentiated HCC cases was seen in the ring-type subgroup [6/37 (16%), Figure 1C] than in the whole-type subgroup [0/37 (0%), Figure 1D]. Tumor differentiation and fibrosis in non-cancerous liver parenchyma could affect ICG FI in HCC. ICG FI may be a good indicator of fibrosis stage.

Intraoperative ICG-FI in hepatic tumors is useful for identifying subcapsular lesions for removal during laparoscopic hepatectomy, in which visual inspection and palpation are limited compared with open surgery (24). This technique has potential drawbacks, however, including a relatively high false-positive rate (14, 20). Lesions that are newly detected by ICG-FI should be resected only when other modalities, such as palpation and intraoperative US, identify them as tumors to be removed. The incidence of false positives can be reduced by not administering ICG on the day before surgery, especially in patients with decreased liver function due to cirrhosis or pre-operative chemotherapy (14). Detecting liver tumors through ICG FI involves visualizing cholestasis inside or around liver cancer because ICG FI does not truly image cancer cells. When new fluorescent regions are visualized during surgery, palpation and US for liver tumors should be performed. Additional resection should be considered if these extra methods suggest malignancies. As ICG FI is also limited in its observation depth

Abbreviations: 5-ALA, 5-aminolevulinic acid; CLRM, colorectal liver metastasis; CT, computed tomography; FI, fluorescence imaging; HC, high cancerous (fluorescence in cancerous tissue); HS, high surrounding (fluorescence in surrounding tissue); ICG, indocyanine green; ICG-L, ICG-lactosome; ICGR15, ICG retention rate at 15 min; MRI, magnetic resonance imaging; NIR, near-infrared; PDT, photodynamic therapy; US, ultrasonography.



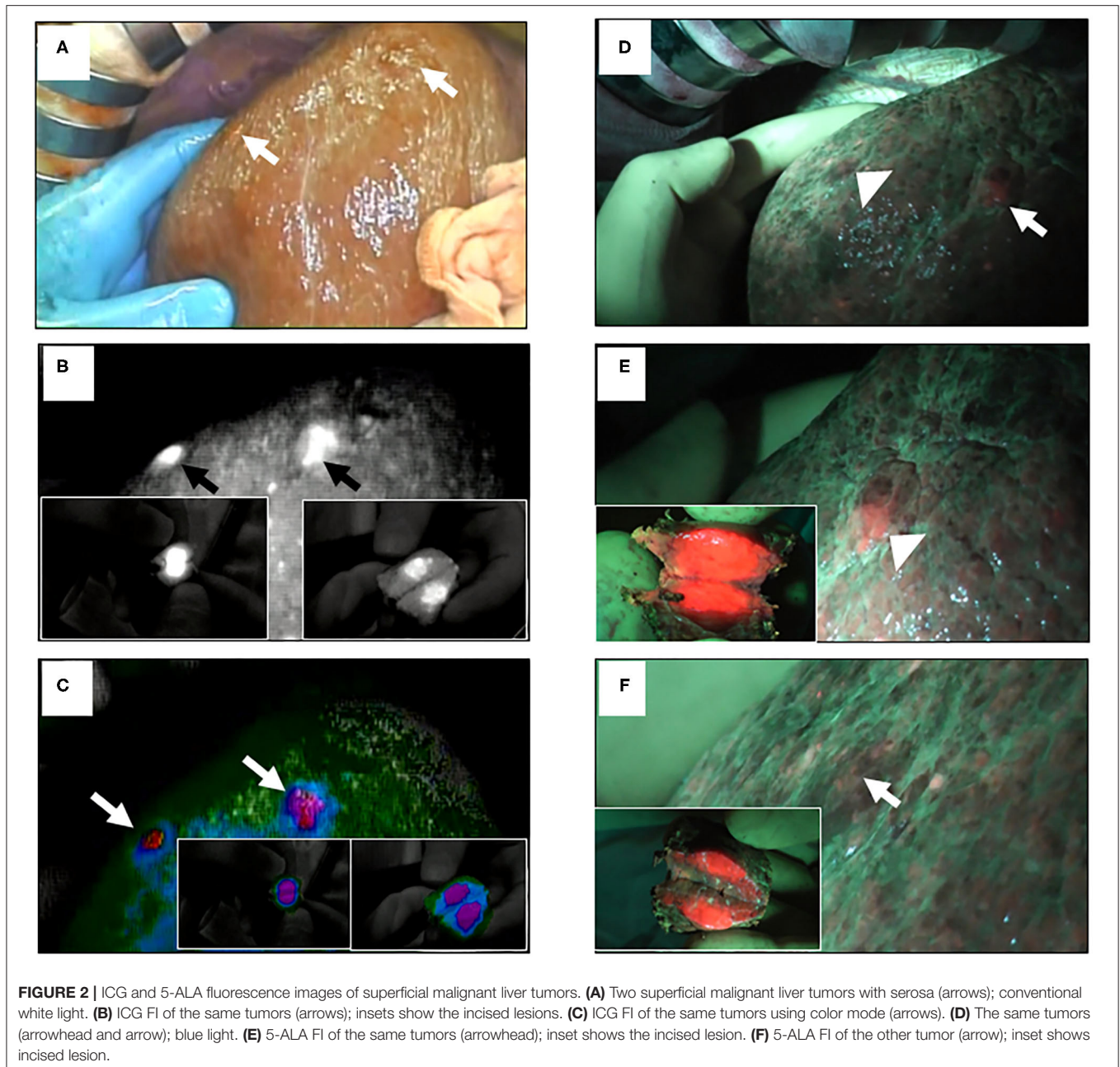
(up to about 8 mm), intraoperative US is required to confirm findings that lie deeper in the liver.

By using ICG and 5-ALA FI, the latent, superficial, and small liver tumors were detected and treated pre-operatively and/or intraoperatively, as we reported previously (25). 5-ALA is a natural precursor of heme, and is accumulated and converted to protoporphyrin IX, which emits red fluorescence in cancer cells (26). Thus, 5-ALA is used as a photosensitizer in photodynamic diagnostics for neurosurgery and urology (27–30). Imaging with ICG or 5-ALA detected small latent liver tumors (Figure 2) and peritoneal dissemination (Figure 3). We conducted a study with 48 patients who had primary liver tumors within 5 mm of the liver surface. With ICG, the sensitivity, specificity, and accuracy for detecting the pre-operatively identified primary tumors were 96, 50, and 94%, respectively. Twelve latent, small tumors were newly detected on the liver surface using ICG. Five of these tumors were determined to be carcinomas. With 5-ALA, the sensitivity, specificity, and accuracy for detecting the primary tumors were 57, 100, and 58%, respectively. Five latent, small tumors were newly detected using 5-ALA; all were carcinomas. Overall, five new tumors were detected by both ICG and 5-ALA FI: two were HCCs and three were metastases of colorectal cancer. The sensitivity and specificity of ICG FI for primary tumor detection were relatively high and low, respectively, but the opposite was true for 5-ALA imaging. In another study, Inoue et al. reported that there was 100% sensitivity for detecting HCC, 86% for colorectal liver metastases, and 100% for liver tumors of various etiologies. 5-ALA showed an overall sensitivity of 93% for detection in their experience with a series of 70 patients who underwent hepatic resection (31). However, Boogerd et al. reported that their study was designed to compare FI and conventional imaging modalities for laparoscopic detection of both primary and metastatic

tumors in the liver (32). Sensitivity for various modalities was 80% (CT), 84% (MRI), 62% (inspection), 86% (laparoscopic ultrasonography), and 92% (ICG-FI). All 26 malignancies that were examined could be detected by combining laparoscopic ultrasonography and ICG-FI (100% sensitivity). To the best of our knowledge, our study is the first to detect liver tumors using both ICG and 5-ALA FI. FI using both ICG and 5-ALA may provide greater specificity in detecting surface-invisible liver tumors than using ICG FI alone. Both imaging methods may help improve treatment strategies for patients with liver tumors.

Cholangiography

Cholangiography is used to visualize the biliary tract intraoperatively to avoid damage to the bile ducts (33). Routine cholangiography is recommended for cholecystectomy (34, 35). A multicenter randomized controlled trial confirmed the superiority of extrahepatic bile-duct identification using ICG fluorescent cholangiography in laparoscopic cholecystectomy (36). Because ICG binds to human bile proteins, such as albumin and lipoproteins (8), intra-bile-duct injection of ICG enables FI of the biliary tract (37). The fluorescent intensity of ICG bound to these proteins was ~ 0.25 mg/mL and correlates with its concentration. However, it was found to decrease at high concentrations from the absorption of near-infrared light by the ICG (5). Therefore, a diluted ICG solution (~ 0.025 mg/mL) should be injected into the bile duct to obtain a clear fluorescent image of the bile duct (31). ICG was detected in the bile duct 20 min after injection and maintained for up to 2 h in patients who underwent laparoscopic cholecystectomy (38, 39). In donor hepatectomy and laparoscopic hepatectomy, ICG cholangiography has been reported (40, 41). Recently, Hong et al. reported that ICG fluorescent cholangiography was successful in delineating the biliary system around the



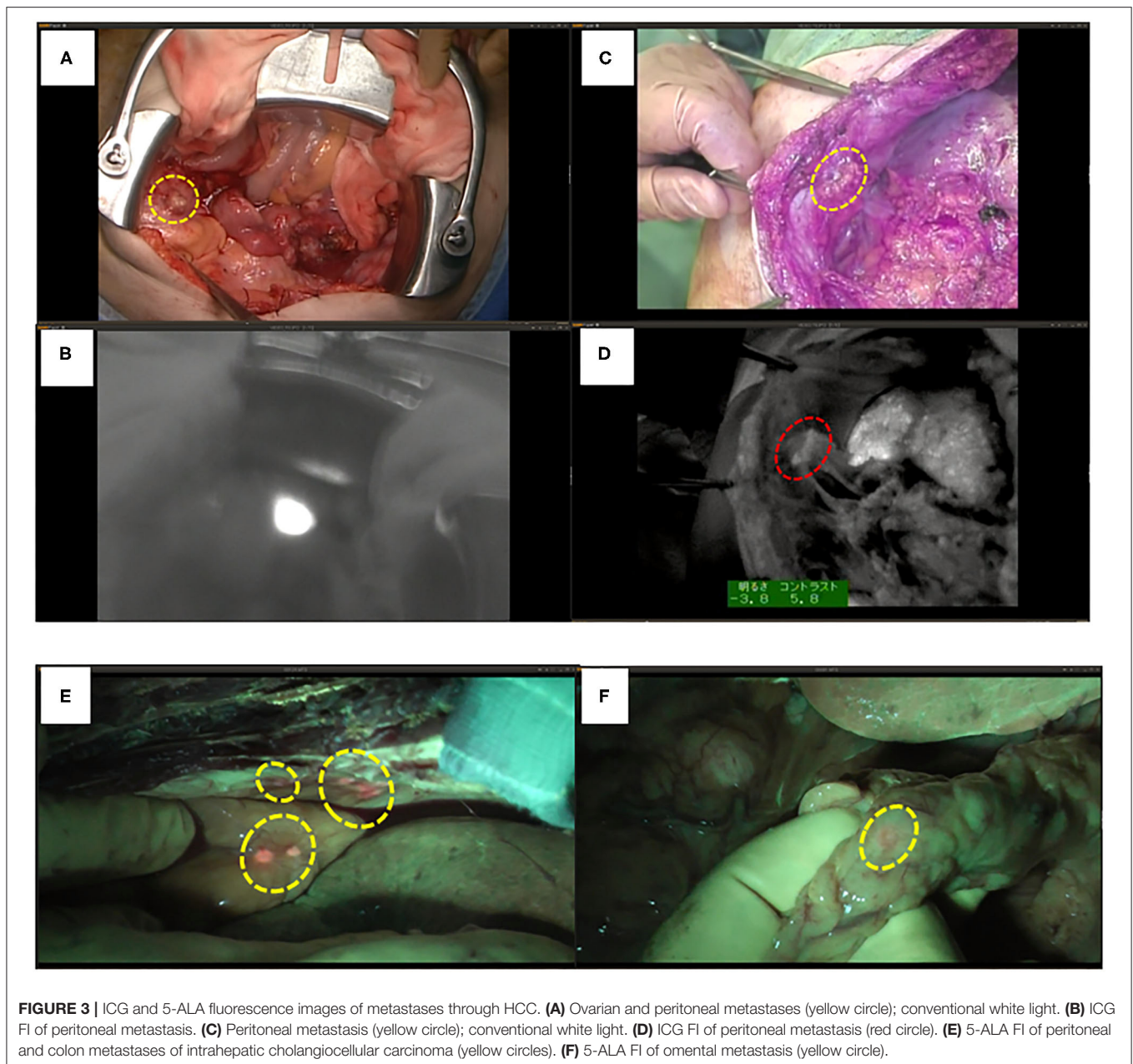
hilar plate and in determining optimal bile duct division points during laparoscopic donor hepatectomy in their ten patients. They suggest that this technique may be particularly useful in laparoscopic surgery, during which intraoperative cholangiography and probing through the divided bile duct opening or cystic duct opening is relatively difficult (42). ICG fluorescent cholangiography is also useful for real-time detection of bile leaks during hepatectomy (43, 44).

We have performed a randomized controlled trial with ICG fluorescence cholangiography in 102 patients who underwent hepatic resection without biliary reconstruction. The patients were divided into two groups: with or without ICG fluorescence cholangiography. In the control group, five patients developed

post-operative bile leakage, but in the ICG cholangiography group, no bile leakage was observed in any patient (10 vs. 0%, $P = 0.019$; **Figure 4**) (44). Thus, ICG cholangiography may help prevent bile leakage. ICG cholangiography also prevented bile leakage and bile duct stenosis in bile duct anastomosis in living-donor liver transplantation (42, 45).

Imaging of Hepatic Segments

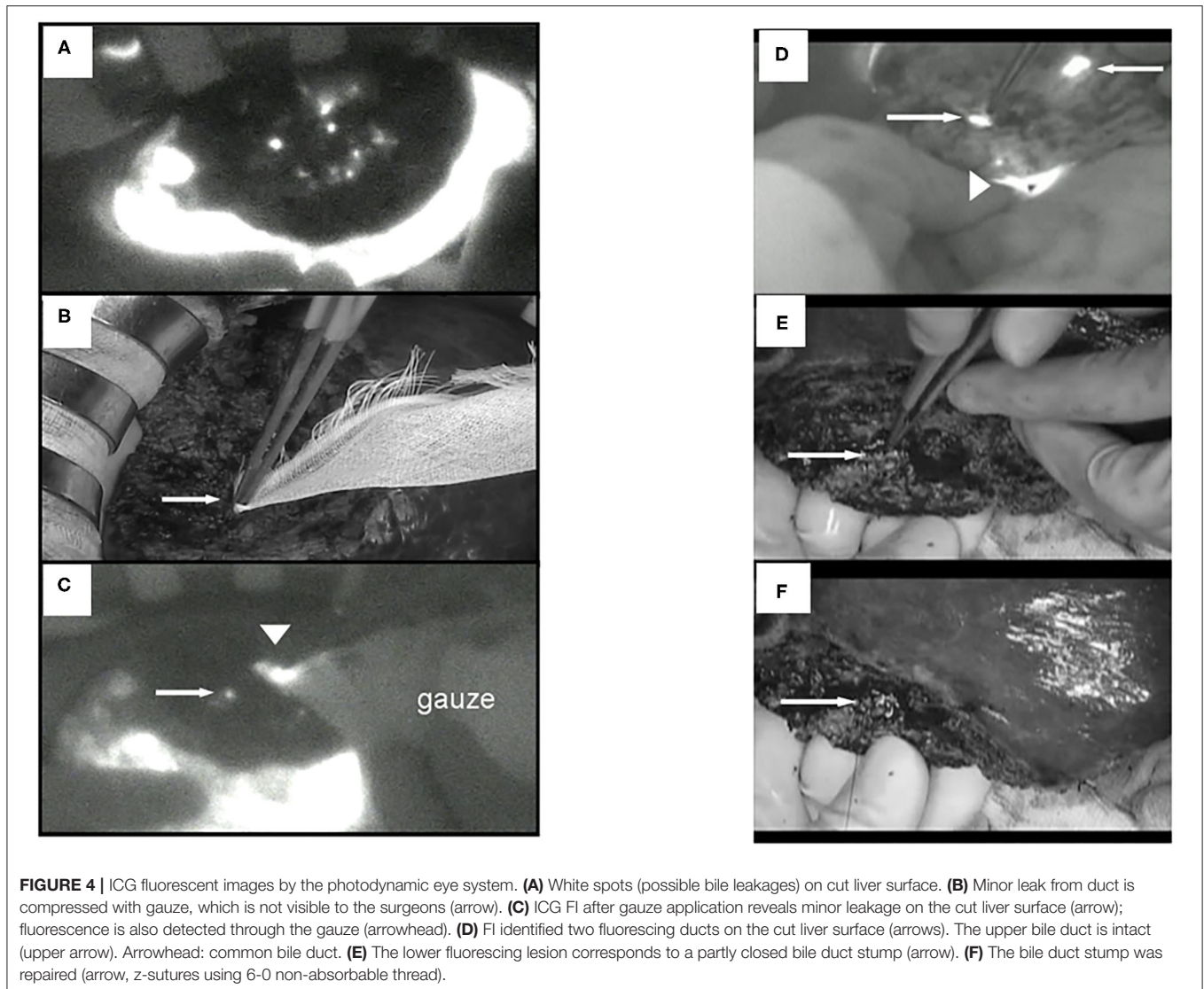
Fusion ICG FI, which displays both fluorescence images and macroscopic views on a single screen, provides clear demarcation lines for more accurate parenchymal dissection (46). Nishino et al. showed that the projection mapping with ICG fluorescence detected anatomical landmarks for parenchymal dissection in



clinical utility (47). Makuuchi et al. first reported anatomical liver resection (48), injecting indigo-carmin into the portal vein, which was followed by some studies of anatomical liver resection using non-anatomical liver resection (49–52). Aoki et al. obtained fluorescence images of the liver surfaces using an infrared camera, after portal vein branches in the HCC-bearing hepatic segment were punctured by intraoperative US (53, 54). They reported that the ICG-staining technique showed the sub-segments and segments in 90% (73/81) of patients, and that there were no differences in detection rates for liver segment boundaries between non-cirrhotic and cirrhotic livers.

Laparoscopic liver resection for HCC was established and became a standard treatment for minor liver resection (55). It

is also performed in specialized centers for laparoscopic liver surgery (56). Ishizawa et al. used the ICG staining technique for laparoscopic anatomical resection (57). Ueno et al. used laparoscopic liver segmentation by interventional radiology technique (58). Although the ICG FI method is a relatively simple method, in the positive staining method when there are multiple dominant portal vein branches or when it is difficult to puncture a thin vessel of 2 mm or less, it is not possible to accurately visualize the hepatic segments. In the negative staining method, prior treatment of the dominant portal vein branch is required, but it is necessary to carefully perform the peeling operation while paying sufficient attention to vascular and bile duct injury (59). Additionally, unlike indigo-carmin which disappears in a



short time, the fluorescent region from ICG is maintained for a long time, so it is difficult to correct the stained region when it is incorrect. To obtain the desired accurate ICG FI during the operation, it is important to perform sufficient simulation before surgery and carefully plan the appropriate ICG FI method for each case.

ICG FI can apparently be safe and reliable for hepatectomy at many facilities and is expected to help improve liver cancer treatment, though its usefulness should be verified in a large-scale, multicenter study.

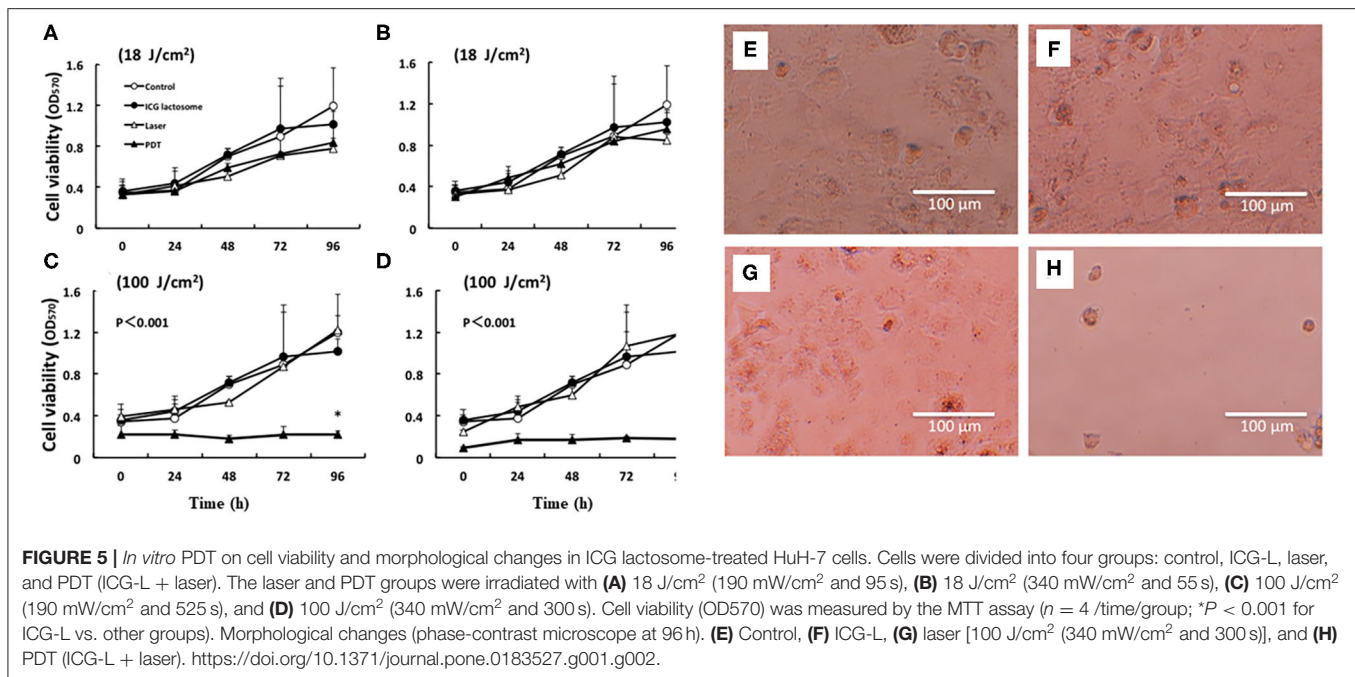
PHOTODYNAMIC THERAPY FOR LIVER TUMORS

Indocyanine Green-Lactosome Has Anti-neoplastic Effects for HCC

We have developed a macromolecular micelle (ICG-lactosome, ICG-L) formed by self-assembly of a novel amphiphatic

polydepsipeptide (containing hydrophilic and hydrophobic parts). ICG-L does not accumulate very much in internal organs because of the stealth effect, but it selectively accumulates in cancer tissues with higher concentration because of the enhanced permeability and retention effect (60). In polydepsipeptide, polysarcosine constitutes the hydrophilic portion, comprises amino acids found in living tissue, and has hydrophilicity equal to or greater than that of polyethylene glycol. It is biodegradable and is widely used in industrial and medical materials. In contrast, polylactic acid is the hydrophobic portion, also biodegradable and used as a medical material, frequently in bone resorbable applications. Compared with other conventional biocompatible nanoparticles, ICG-L is easy to use in designed products. Its particle sizes can be adjusted and modified with biomaterials such as peptides; it may work as a carrier for “theranostic” diagnostic agents and pharmaceuticals (61).

For the evaluation of PDT efficacy *in vitro*, HuH-7 (human HCC cell line) cells were treated with ICG-L or ICG, followed by PDT. The cell viabilities were then measured. Laser irradiation



revealed that HuH-7 cells with ICG-L showed toxic effects, but the cells with ICG alone did not (Figure 5).

For NIF *in vivo*, BALB/c nude mice were subcutaneously treated with HuH-7 cells and then intravenously with ICG-L or ICG. These transplanted animals were treated with PDT and the antineoplastic effects were analyzed. Indeed, NIF imaging revealed that the tumor-area fluorescence in ICG-L-treated animals was higher than that of contralateral regions at 24 h after injection and thereafter (Figures 6B,D), although there was no difference between those in the tumor-area fluorescence in ICG-treated animals (Figures 6A,C). PDT had continuous phototoxic effects in the ICG-L group (Figure 7A). By laser irradiation, the median temperature in the tumor areas increased from 34 to 47.7°C and from 34.5 to 51.7°C at 0–200 s in the ICG-L and ICG groups, respectively (Figure 6E), where the median temperature in the ICG-L group was higher than that in the ICG group.

In the former, there was substantial apoptosis with a higher apoptotic index in the ICG-L group than in the ICG group (Figures 7B–D). The mechanisms involved in tumor suppression by PDT in the ICG-L group were presumably caused by singlet oxygen and ICG degradation products generated by a photochemical reaction (62). Singlet oxygen can be generated as ICG is exposed to near-infrared excitation light. The decomposition products that can be produced by ICG can further decrease cell viability (63). These products may lead to tumor cell apoptosis. PDT with ICG-L increased the tumor suppression by the heat generated from a photothermal reaction. During *in vivo* analysis of PDT with ICG-L, the temperature increased (50°C and above) relative to ICG alone, suggesting that the heat may be sufficient to damage tumor growth. In addition, optimization of ICG-L dosage and laser irradiation fluence are also necessary

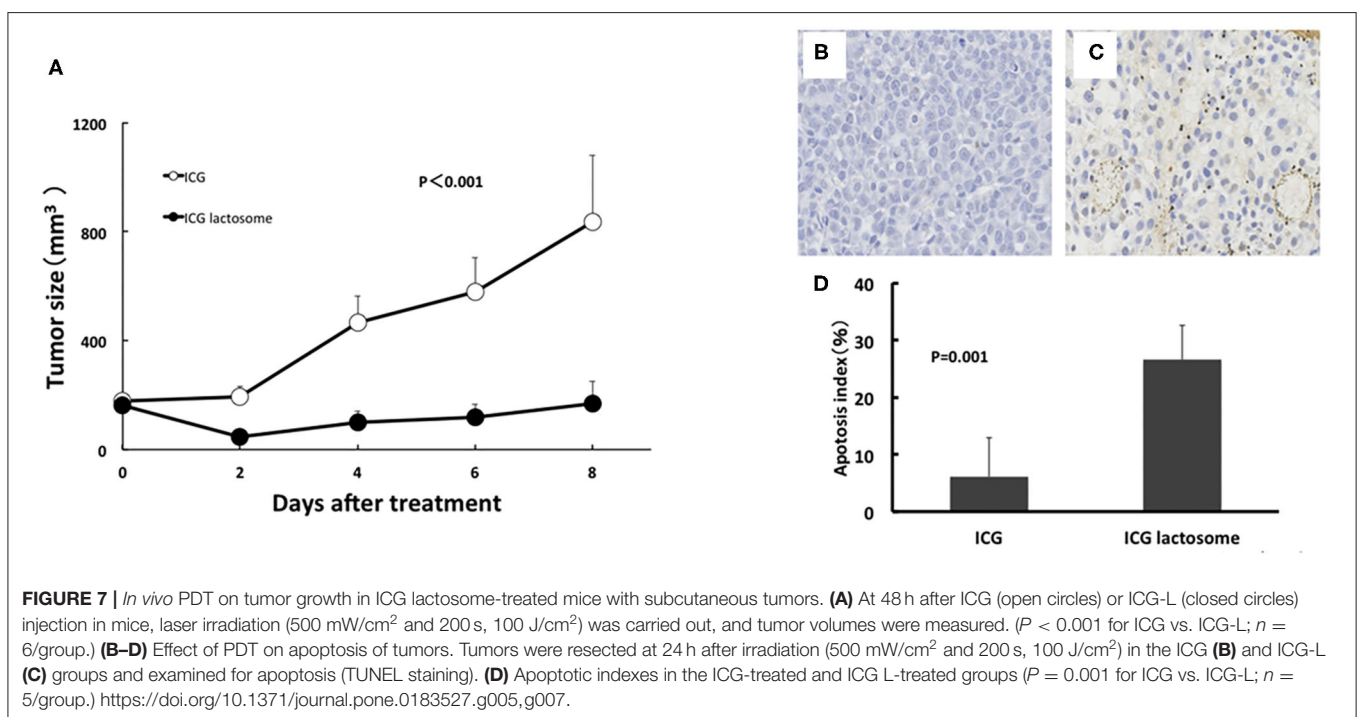
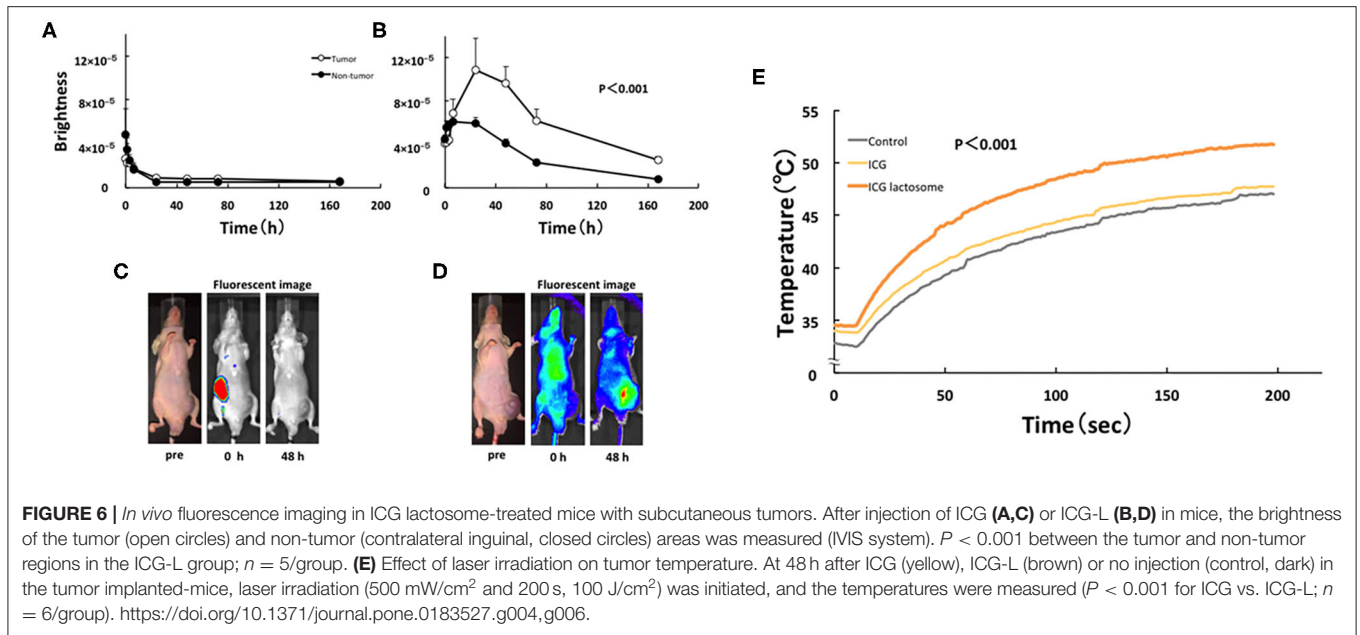
to prevent future tumor growth. The temperature increase is a major factor in the antitumor effect obtained in our study because PDT using ICG reportedly has a thermal effect (64). The temperature increase by PDT likely depends on various photosensitizers, including ICG. PDT using ICG can facilitate a temperature increase with antitumor effects, which supports the usefulness of ICG-L.

Our results demonstrated that tumor cells transplanted in BALB/c nude mice incorporated ICG-L and that PDT had antineoplastic effects. NIF imaging and PDT with ICG-L may be useful diagnostic and/or therapeutic strategies for HCC.

There are some limitations to ICG FI. First, ICG-L may possibly accumulate in both malignant and benign tumors, causing excessive influence in undesired areas by PDT. There is little knowledge regarding angiogenesis in benign tumors compared with in malignant tumors. Because benign tumors generally have slower growth rates and do not infiltrate into other tissues compared with malignant tumors, we believe it would be difficult to integrate ICG-L into benign tumors.

In clinical situations, Ishizawa et al. reported that ICG FI can be used to observe HCC lesions based on their tumorous fluorescence. This is because the portal uptake of ICG is preserved in well- or moderately differentiated cancer tissues, despite the lack of biliary extraction and to delineate poorly differentiated HCC as rim-fluorescing lesions because of biliary excretion disorders in the surrounding non-cancerous liver tissues that are compressed by the tumor (14).

The second limitation is that it is not clear how the PDT effect of ICG-L depends on the tumor differentiation, tumor size, and depth from the liver surface. We have only investigated the Huh-7 cell line as well-differentiated HCC. ICG-L (excitation



wavelength: 774 nm , fluorescence wavelength: 805 nm) reaches a depth of $10\text{--}20 \text{ mm}$ subcutaneously in the near infrared region ($700\text{--}1000 \text{ nm}$) (60, 61). Future studies are needed on the PDT effect of ICG-L on the tumor diameter and degree of HCC differentiation.

Funayama et al. (65–67) reported that PDF with ICG-L delayed the development of paralysis in rats with spinal metastases. Tsujimoto et al. (68, 69) reported that PDF with ICG-L inhibited the growth of metastases. Recently, we found

an antitumor effect of PT with ICG-L on gallbladder cancer in xenograft tumors (70). In other experiments, Kaneko et al. (71, 72) reported using PDT with ICG and an NIR laser for HCC. HuH-7 cells were transplanted subcutaneously into BALB/c-*nu/nu* mice and ICG was administered 24 h before NIR irradiation (days 1 and 7). Repeated NIR increased the cell toxicity of ICG-NIR therapy. They also found that ICG-NIR therapy increased apoptosis in tumor cells through a photothermal effect and oxidative stress.

CONCLUSIONS

ICG FI has effects on fibrosis detection and tumor differentiation measurement in non-cancerous liver parenchyma in HCC. ICG FI can be a good indicator of fibrosis stage and apparently detect smaller liver tumors. FI with 5-ALA provided higher specificity in detecting surface-invisible liver tumors as compared with FI with ICG. Usage of both ICG and 5-ALA imaging can potentially improve treatment strategies for patients with liver tumors. Simply put, FI offers the benefits of a higher-resolution intraoperative navigation tool for liver cancer. ICG-L is useful as a diagnostic and therapeutic agent for HCC.

REFERENCES

- Rubens FD, Ruel M, Frenes SE. A new and simplified method for coronary and graft imaging during CABG. *Heart Surg Forum.* (2002) 5:141–4.
- Taggart DP, Choudhary B, Anastasiadis K, Abu-Omar Y, Balacumaraswani L, Pigott DW. Preliminary experience with a novel intraoperative fluorescence imaging technique to evaluate the patency of bypass grafts in total arterial revascularization. *Ann Thorac Surg.* (2003) 75:870–3. doi: 10.1016/S0003-4975(02)04669-6
- Reuthebuch O, Haussler A, Genoni M, Tavakoli R, Odavic D, Kadner A, et al. Intraoperative quality assessment in off-pump coronary artery bypass grafting. *Chest.* (2004) 125:418–24. doi: 10.1378/chest.125.2.418
- Balacumaraswani L, Abu-Omar Y, Choudhary B, Pigott D, Taggart DP. A comparison of transit-time flowmetry and intraoperative fluorescence imaging for assessing coronary artery bypass graft patency. *J Thorac Cardiovasc Surg.* (2005) 130:315–20. doi: 10.1016/j.jtcvs.2004.11.033
- Mitsuhashi N, Kimura F, Shimizu H, Imamaki M, Yoshidome H, Ohtsuka M, et al. Usefulness of intraoperative fluorescence imaging to evaluate local anatomy in hepatobiliary surgery. *J Hepatobiliary Pancreat Surg.* (2008) 15:508–14. doi: 10.1007/s00534-007-1307-5
- Landsman ML, Kwant G, Mook GA, Zijlstra WG. Light-absorbing properties, stability, and spectral stabilization of indocyanine green. *J Appl Physiol.* (1976) 40:575–83. doi: 10.1152/jappl.1976.40.4.575
- Mordon S, Devoisselle JM, Soulie-Begu S, Desmetre T. Indocyanine green: physicochemical factors affecting its fluorescence *in vivo*. *Microvasc Res.* (1998) 55:146–52. doi: 10.1006/mvrc.1998.2068
- Mullock BM, Shaw LJ, Fitzharris B, Peppard J, Hamilton MJ, Simpson MT, et al. Sources of proteins in human bile. *Gut.* (1985) 26:500–9. doi: 10.1136/gut.26.5.500
- Makuuchi M, Kosuge T, Takayama T, Yamazaki S, Kakazu T, Miyagawa S, et al. Surgery for small liver cancers. *Semin Surg Oncol.* (1993) 9:298–304. doi: 10.1002/ssu.2980090404
- Ishizawa T, Hasegawa K, Aoki T, Takahashi M, Inoue Y, Sano K, et al. Neither multiple tumors nor portal hypertension are surgical contraindications for hepatocellular carcinoma. *Gastroenterology.* (2008) 134:1908–16. doi: 10.1053/j.gastro.2008.02.091
- Xie J, Lee S, Chen X. Nanoparticle-based theranostic agents. *Adv Drug Deliv Rev.* (2010) 62:1064–79. doi: 10.1016/j.addr.2010.07.009
- Matsumura Y, Maeda H. A new concept for macromolecular therapeutics in cancer chemotherapy: mechanism of tumoritropic accumulation of proteins and the antitumor agent smancs. *Cancer Res.* (1986) 46:6387–92.
- Gotoh K, Yamada T, Ishikawa O, Takahashi H, Eguchi H, Yano M, et al. A novel image-guided surgery of hepatocellular carcinoma by indocyanine green fluorescence imaging navigation. *J Surg Oncol.* (2009) 100:75–9. doi: 10.1002/jso.21272
- Ishizawa T, Fukushima N, Shibahara J, Masuda K, Tamura S, Aoki T, et al. Real-time identification of liver cancers by using indocyanine green fluorescent imaging. *Cancer.* (2009) 115:2491–504. doi: 10.1002/cncr.24291
- Peloso A, Franchi E, Canepa MC, Barbieri L, Briani L, Ferrario J, et al. Combined use of intraoperative ultrasound and indocyanine green

PDT using ICG-L, which is repeatedly performed, can be used in endoscopic or laparoscopic therapy for small HCC tumors. To develop PDT with FI in clinical applications, we will examine optimal drug dosages, irradiation conditions, and the effects of treatment on other carcinomas.

AUTHOR CONTRIBUTIONS

MK drafted and wrote the manuscript. HM, MI, HK, KM, TT, HH, TO, and MS participated in the study design and helped draft the manuscript. All authors contributed to the interpretation of the findings, read, and approved the final manuscript.

- fluorescence imaging to detect liver metastases from colorectal cancer. *HPB (Oxford).* (2013) 15:928–34. doi: 10.1111/hpb.12057
- Terasawa M, Ishizawa T, Mise Y, Inoue Y, Ito H, Takahashi Y, et al. Applications of fusion-fluorescence imaging using indocyanine green in laparoscopic hepatectomy. *Surg Endosc.* (2017) 31:5111–8. doi: 10.1007/s00464-017-5576-z
 - Miyazaki Y, Kurata M, Oshiro Y, Shimomura O, Takahashi K, Oda T, et al. Indocyanine green fluorescence-navigated laparoscopic metastasectomy for peritoneal metastasis of hepatocellular carcinoma: a case report. *Surg Case Rep.* (2018) 4:130. doi: 10.1186/s40792-018-0537-x
 - Nakamura M, Hayami S, Ueno M, Kawai M, Miyamoto A, Suzuki N, et al. Detection of needle tract implantation and peritoneal seeding after radiofrequency ablation using intraoperative near-infrared fluorescence system for recurrent hepatocellular carcinoma: a case report. *Surg Case Rep.* (2018) 4:76. doi: 10.1186/s40792-018-0485-5
 - Satou S, Ishizawa T, Masuda K, Kaneko J, Aoki T, Sakamoto Y, et al. Indocyanine green fluorescent imaging for detecting extrahepatic metastasis of hepatocellular carcinoma. *J Gastroenterol.* (2013) 48:1136–43. doi: 10.1007/s00535-012-0709-6
 - Ishizawa T, Masuda K, Urano Y, Kawaguchi Y, Satou S, Kaneko J, et al. Mechanistic background and clinical applications of indocyanine green fluorescence imaging of hepatocellular carcinoma. *Ann Surg Oncol.* (2014) 21:440–8. doi: 10.1245/s10434-013-3360-4
 - de Graaf W, Häusler S, Heger M, van Ginhoven TM, van Cappellen G, Bennink RJ, et al. Transporters involved in the hepatic uptake of (99m)Tc-mebrofenin and indocyanine green. *J Hepatol.* (2011) 54:738–45. doi: 10.1016/j.jhep.2010.07.047
 - van der Vorst JR, Schaafsma BE, Hutteman M, Verbeek FP, Liefers GJ, Hartgrink HH, et al. Nearinfrared fluorescence-guided resection of colorectal liver metastases. *Cancer.* (2013) 119:3411–8. doi: 10.1002/cncr.28203
 - Kaibori M, Matsui K, Ishizaki M, Iida H, Sakaguchi T, Tsuda T, et al. Evaluation of fluorescence imaging with indocyanine green in hepatocellular carcinoma. *Cancer Imaging.* (2016) 16:6. doi: 10.1186/s40644-016-0064-6
 - Kudo H, Ishizawa T, Tani K, Harada N, Ichida A, Shimizu A, et al. Visualization of subcapsular hepatic malignancy by indocyanine-green fluorescence imaging during laparoscopic hepatectomy. *Surg Endosc.* (2014) 28:2504–8. doi: 10.1007/s00464-014-3468-z
 - Kaibori M, Matsui K, Ishizaki M, Iida H, Okumura T, Sakaguchi T, et al. Intraoperative detection of superficial liver tumors by fluorescence imaging using indocyanine green and 5-aminolevulinic acid. *Anticancer Res.* (2016) 36:1841–9.
 - Ohgari Y, Nakayasu Y, Kitajima S, Sawamoto M, Mori H, Shimokawa O, et al. Mechanisms involved in delta-aminolevulinic acid (ALA)-induced photosensitivity of tumor cells: relation of ferrochelatase and uptake of ALA to the accumulation of protoporphyrin. *Biochem Pharmacol.* (2005) 71:42–9. doi: 10.1016/j.bcp.2005.10.019
 - Kriegmair M, Baumgartner R, Knüchel R, Stepp H, Hofstädter F, Hofstetter A. Detection of early bladder cancer by 5-aminolevulinic acid induced porphyrin fluorescence. *J Urol.* (1996) 155:105–9. doi: 10.1016/S0022-5347(01)66559-5

28. Jichlinski P, Forrer M, Mizeret J, Glanzmann T, Braichotte D, Wagnières G, et al. Clinical evaluation of a method for detecting superficial surgical transitional cell carcinoma of the bladder by light-induced fluorescence of protoporphyrin IX following the topical application of 5-aminolevulinic acid: preliminary results. *Lasers Surg Med.* (1997) 20:402–8. doi: 10.1002/(SICI)1096-9101(1997)20:4<402::AID-LSM5>3.0.CO;2-U
29. Stummer W, Stocker S, Wagner S, Stepp H, Fritsch C, Goetz C, et al. Intraoperative detection of malignant gliomas by 5-aminolevulinic acid-induced porphyrin fluorescence. *Neurosurgery.* (1998) 42:518–26. doi: 10.1097/00006123-199803000-00017
30. Friesen SA, Hjortland GO, Madsen SJ, Hirschberg H, Engebraten O, Nesland JM, et al. 5-Aminolevulinic acid-based photodynamic detection and therapy of brain tumors. *Int J Oncol.* (2002) 21:577–82. doi: 10.3892/ijo.21.3.577
31. Inoue Y, Tanaka R, Komeda K, Hirokawa F, Hayashi M, Uchiyama K. Fluorescence detection of malignant liver tumors using 5-aminolevulinic acid-mediated photodynamic diagnosis: principles, technique, and clinical experience. *World J Surg.* (2014) 38:1786–94. doi: 10.1007/s00268-014-2463-9
32. Boogerd LS, Handgraaf HJ, Lam HD, Huurman VA, Farina-Sarasqueta A, Frangioni JV, et al. Laparoscopic detection and resection of occult liver tumors of multiple cancer types using real-time near-infrared fluorescence guidance. *Surg Endosc.* (2017) 31:952–61. doi: 10.1007/s00464-016-5007-6
33. Waage A, Nilsson M. Iatrogenic bile duct injury: a population-based study of 152 776 cholecystectomies in the Swedish inpatient registry. *Arch Surg.* (2006) 141:1207–13. doi: 10.1001/archsurg.141.12.1207
34. Rystedt JML, Tingstedt B, Montgomery F, Montgomery AK. Routine intraoperative cholangiography during cholecystectomy is a cost-effective approach when analysing the cost of iatrogenic bile duct injuries. *HPB (Oxford).* (2017) 19:881–8. doi: 10.1016/j.hpb.2017.06.004
35. Jeng KS, Huang CC, Lin CK, Lin CC, Chen KH, Chu SH. Repeated intraoperative cholangiography is helpful for donor safety in the procurement of right liver graft with supraportal right bile duct variants in living-donor liver transplantation. *Transplant Proc.* (2014) 46:686–8. doi: 10.1016/j.transproceed.2013.11.093
36. Dip F, LoMenzo E, Sarotto L, Phillips E, Todeschini H, Nahmod M, et al. Randomized trial of near-infrared incisionless fluorescent cholangiography. *Ann Surg.* (2019) 270:992–9. doi: 10.1097/SLA.0000000000003178
37. Ishizawa T, Tamura S, Masuda K, Aoki T, Hasegawa K, Imamura H, et al. Intraoperative fluorescent cholangiography using indocyanine green: a biliary road map for safe surgery. *J Am Coll Surg.* (2009) 208:e1–4. doi: 10.1016/j.jamcollsurg.2008.09.024
38. Schols RM, Bouvy ND, van Dam RM, Masclee AA, Dejong CH, Stassen LP. Combined vascular and biliary fluorescence imaging in laparoscopic cholecystectomy. *Surg Endosc.* (2013) 27:4511–7. doi: 10.1007/s00464-013-3100-7
39. Kaneko J, Ishizawa T, Masuda K, Kawaguchi Y, Aoki T, Sakamoto Y, et al. Indocyanine green reinjection technique for use in fluorescent angiography concomitant with cholangiography during laparoscopic cholecystectomy. *Surg Laparosc Endosc Percutan Tech.* (2012) 22:341–4. doi: 10.1097/SLE.0b013e3182570240
40. Mizuno S, Isaji S. Indocyanine green (ICG) fluorescence imaging-guided cholangiography for donor hepatectomy in living donor liver transplantation. *Am J Transplant.* (2010) 10:2725–6. doi: 10.1111/j.1600-6143.2010.03288.x
41. Kawaguchi Y, Velayutham V, Fuks D, Christidis C, Kokudo N, Gayet B. Usefulness of indocyanine green-fluorescence imaging for visualization of the bile duct during laparoscopic liver resection. *J Am Coll Surg.* (2015) 221:e113–7. doi: 10.1016/j.jamcollsurg.2015.09.001
42. Hong SK, Lee KW, Kim HS, Yoon KC, Ahn SW, Choi JY, et al. Optimal bile duct division using real-time indocyanine green near-infrared fluorescence cholangiography during laparoscopic donor hepatectomy. *Liver Transpl.* (2017) 23:847–52. doi: 10.1002/lt.24686
43. Diana M, Usmaan H, Legner A, Yin LY, D'Urso A, Halvax P, et al. Novel laparoscopic narrow band imaging for real-time detection of bile leak during hepatectomy: proof of the concept in a porcine model. *Surg Endosc.* (2016) 30:3128–32. doi: 10.1007/s00464-015-4569-z
44. Kaibori M, Ishizaki M, Matsui K, Kwon AH. Intraoperative indocyanine green fluorescent imaging for prevention of bile leakage after hepatic resection. *Surgery.* (2011) 150:91–8. doi: 10.1016/j.surg.2011.02.011
45. Mizuno S, Inoue H, Tanemura A, Murata Y, Kuriyama N, Azumi Y, et al. Biliary complications in 108 consecutive recipients with duct-to-duct biliary reconstruction in living-donor liver transplantation. *Transplant Proc.* (2014) 46:850–5. doi: 10.1016/j.transproceed.2013.11.035
46. Inoue Y, Arita J, Sakamoto T, Ono Y, Takahashi M, Takahashi Y, et al. Anatomical liver resections guided by 3-dimensional parenchymal staining using fusion indocyanine green fluorescence imaging. *Ann Surg.* (2015) 262:105–11. doi: 10.1097/SLA.0000000000000775
47. Nishino H, Hatano E, Seo S, Nitta T, Saito T, Nakamura M, et al. Real-time navigation for liver surgery using projection mapping with indocyanine green fluorescence: development of the novel medical imaging projection system. *Ann Surg.* (2018) 267:1134–40. doi: 10.1097/SLA.0000000000002172
48. Makuuchi M, Hasegawa H, Yamazaki S. Ultrasonically guided subsegmentectomy. *Surg Gynecol Obstet.* (1985) 161:346–50.
49. Jung DH, Hwang S, Lee YJ, Kim KH, Song GW, Ahn CS, et al. Small hepatocellular carcinoma with low tumor marker expression benefits more from anatomical resection than tumors with aggressive biology. *Ann Surg.* (2019) 269:511–9. doi: 10.1097/SLA.0000000000002486
50. Shindoh J, Makuuchi M, Matsuyama Y, Mise Y, Arita J, Sakamoto Y, et al. Complete removal of the tumor-bearing portal territory decreases local tumor recurrence and improves disease-specific survival of patients with hepatocellular carcinoma. *J Hepatol.* (2016) 64:594–600. doi: 10.1016/j.jhep.2015.10.015
51. Kaibori M, Kon M, Kitawaki T, Kawaura T, Hasegawa K, Kokudo N, et al. Comparison of anatomic and non-anatomic hepatic resection for hepatocellular carcinoma. *J Hepatobiliary Pancreat Sci.* (2017) 24:616–26. doi: 10.1002/jhbp.502
52. Kaibori M, Yoshii K, Hasegawa K, Ariizumi S, Kobayashi T, Kamiyama T, et al. Impact of systematic segmentectomy for small hepatocellular carcinoma. *J Hepatobiliary Pancreat Sci.* (2020) 27:331–41. doi: 10.1002/jhbp.720
53. Aoki T, Yasuda D, Shimizu Y, Odaira M, Niiya T, Kusano T, et al. Image-guided liver mapping using fluorescence navigation system with indocyanine green for anatomical hepatic resection. *World J Surg.* (2008) 32:1763–7. doi: 10.1007/s00268-008-9620-y
54. Aoki T, Murakami M, Yasuda D, Shimizu Y, Kusano T, Matsuda K, et al. Intraoperative fluorescent imaging using indocyanine green for liver mapping and cholangiography. *J Hepatobiliary Pancreat Sci.* (2010) 17:590–4. doi: 10.1007/s00534-009-0197-0
55. Ciria R, Cherqui D, Geller DA, Briceno J, Wakabayashi G. Comparative short-term benefits of laparoscopic liver resection: 9000 cases and climbing. *Ann Surg.* (2016) 263:761–77. doi: 10.1097/SLA.0000000000001413
56. Wakabayashi G, Cherqui D, Geller DA, Buell JF, Kaneko H, Han HS, et al. Recommendations for laparoscopic liver resection: a report from the second international consensus conference held in Morioka. *Ann Surg.* (2015) 261:619–29. doi: 10.1097/SLA.0000000000001184
57. Ishizawa T, Zuker NB, Kokudo N, Gayet B. Positive and negative staining of hepatic segments by use of fluorescent imaging techniques during laparoscopic hepatectomy. *Arch Surg.* (2012) 147:393–4. doi: 10.1001/archsurg.2012.59
58. Ueno M, Hayami S, Sonomura T, Tanaka R, Kawai M, Hirono S, et al. Indocyanine green fluorescence imaging techniques and interventional radiology during laparoscopic anatomical liver resection (with video). *Surg Endosc.* (2018) 32:1051–5. doi: 10.1007/s00464-017-5997-8
59. Aoki T, Koizumi T, Mansour DA, Fujimori A, Kusano T, Matsuda K, et al. Ultrasound-guided preoperative positive percutaneous indocyanine green fluorescence staining for laparoscopic anatomical liver resection. *J Am Coll Surg.* (2020) 230:e7–12. doi: 10.1016/j.jamcollsurg.2019.11.004
60. Butcher NJ, Mortimer GM, Minchin RF. Unravelling the stealth effect. *Nat Nanotechnol.* (2016) 11:310–1. doi: 10.1038/nnano.2016.6
61. Tsuda T, Kaibori M, Hishikawa H, Nakatake R, Okumura T, Ozeki E, et al. Near-infrared fluorescence imaging and photodynamic therapy with indocyanine green lactosome has antineoplastic effects for hepatocellular carcinoma. *PLoS ONE.* (2017) 12:e0183527. doi: 10.1371/journal.pone.0183527
62. Engel E, Schraml R, Maisch T, Kobuch K, Konig B, Szeimies R, et al. Light-induced decomposition of indocyanine green. *Invest Ophthalmol Vis Sci.* (2008) 49:1777–83. doi: 10.1167/iovs.07-0911

63. Hirano T, Kohno E, Gohto Y, Obana A. Singlet oxygen generation by irradiation of indocyanine green (ICG) and its effect to tissues. *J Jpn Soc Laser Surg Med.* (2007) 28:122–8. doi: 10.2530/jslsm.28.122
64. Lee YH, Lai YH. Synthesis, characterization, and biological evaluation of anti-HER2 indocyanine green-encapsulated PEG-coated PLGA nanoparticles for targeted phototherapy of breast cancer cells. *PLoS ONE.* (2016) 11:e0168192. doi: 10.1371/journal.pone.0168192
65. Funayama T, Sakane M, Abe T, Ochiai N. Photodynamic therapy with indocyanine green injection and near-infrared light irradiation has phototoxic effects and delays paralysis in spinal metastasis. *Photomed Laser Surg.* (2012) 30:47–53. doi: 10.1089/pho.2011.3080
66. Funayama T, Sakane M, Abe T, Hara I, Ozeki E, Ochiai N. Intraoperative near-infrared fluorescence imaging with novel indocyanine green-loaded nanocarrier for spinal metastasis: a preliminary animal study. *Open Biomed Eng.* (2012) 6:80–4. doi: 10.2174/1874120701206010080
67. Funayama T, Tsukanishi T, Hara I, Ozeki E, Sakane M. Tumor-selective near-infrared photodynamic therapy with novel indocyanine green-loaded nanocarrier delays paralysis in rats with spinal metastasis. *Photodiagnosis Photodyn Ther.* (2013) 10:374–8. doi: 10.1016/j.pdpdt.2013.03.002
68. Tsujimoto H, Morimoto Y, Takahata R, Nomura S, Yoshida K, Horiguchi H, et al. Photodynamic therapy using nanoparticle loaded with indocyanine green for experimental peritoneal dissemination of gastric cancer. *Cancer Sci.* (2014) 105:1626–30. doi: 10.1111/cas.12553
69. Tsujimoto H, Morimoto Y, Takahata R, Nomura S, Yoshida K, Hiraki S, et al. Theranostic photosensitive nanoparticles for lymph node metastasis of gastric cancer. *Ann Surg Oncol.* (2015) 22:S923–8. doi: 10.1245/s10434-015-4594-0
70. Hishikawa H, Kaibori M, Tsuda T, Matsui K, Okumura T, Ozeki E, et al. Near-infrared fluorescence imaging and photodynamic therapy with indocyanine green lactosomes has antineoplastic effects for gallbladder cancer. *Oncotarget.* (2019) 10:5622–31. doi: 10.18632/oncotarget.27193
71. Kaneko J, Inagaki Y, Ishizawa T, Jianjun G, Wei T, Aoki T, et al. Photodynamic therapy for human hepatoma-cell-line tumors utilizing biliary excretion properties of indocyanine green. *J Gastroenterol.* (2014) 49:110–6. doi: 10.1007/s00535-013-0775-4
72. Shirata C, Kaneko J, Inagaki Y, Kokudo T, Sato M, Kiritani S, et al. Near-infrared photothermal/photodynamic therapy with indocyanine green induces apoptosis of hepatocellular carcinoma cells through oxidative stress. *Sci Rep.* (2017) 7:13958. doi: 10.1038/s41598-017-14401-0

Conflict of Interest: The authors declare that the research was conducted in the absence of any commercial or financial relationships that could be construed as a potential conflict of interest.

Copyright © 2021 Kaibori, Kosaka, Matsui, Ishizaki, Matsushima, Tsuda, Hishikawa, Okumura and Sekimoto. This is an open-access article distributed under the terms of the Creative Commons Attribution License (CC BY). The use, distribution or reproduction in other forums is permitted, provided the original author(s) and the copyright owner(s) are credited and that the original publication in this journal is cited, in accordance with accepted academic practice. No use, distribution or reproduction is permitted which does not comply with these terms.